ACTIVE MEDIA

PACS numbers: 42.55.Rz; 42.70.Hj
DOI: 10.1070/QE2010v040n01ABEH014184

Specific features of thermal regimes in rectangular laser slabs under steady-state pumping

A.N. Alpat'ev, V.A. Smirnov, I.A. Shcherbakov

***Abstract*. We continue to investigate the phenomena related to smoothing of temperature profiles in rectangular laser slabs and to an increase in the thresholds of their breakdown under optical pumping with variations in the slab optical density [the effect of smoothing of thermooptical inhomogeneities (STOI effect)]. It is found that the STOI effect is observed not only with increasing but also with decreasing optical density if this occurs due to a decrease in the sample thickness. The dependence of the maximum temperature difference inside the slab on its optical density at the instant of its thermal breakdown is calculated. It is shown that the variations in the optical density caused by variations in both the absorption coefficient and geometric dimensions of the slab differently affect the order of occurrence of two undesirable events – destruction of the slab or boiling of cooling water – with increasing pump power. The calculated relationships reveal two optical density regions corresponding to different orders of occurrence of these events. The maximum allowable temperatures in each region are determined.**

Keywords: *thermal regimes, laser active elements*

1. Introduction

One of the main problems in the creation of lasers with high average powers is the heating of active elements (AEs), which restricts the lasing efficiency due to deterioration of the AE spectroscopic parameters, induces a thermal lens, causes thermal breakdown of the AE, etc. As is known, the use of AEs in the form of rectangular slabs allows one to enhance heat removal by increasing the area of surfaces contacting with the cooling medium.

As was shown in works [1 – 4], an increase in the AE optical density at the pump wavelength causes smoothing of thermooptical inhomogeneities (STOI effect), which manifests itself as a decrease in the laser beam divergence and an increase in the thermal breakdown threshold.

In this paper, we consider the ultimate potentials of AEs in the form of rectangular slabs under steady-state pumping, whose increase either leads to the thermal breakdown of the AE or heats it to a temperature at which the normal cooling regime is impossible (for example, in the case of water cooling, at which the water boils). We determined the dependences of the maximum possible pump radiation intensities not only on the optical density D ($D = kh$), but also on the absorption coefficient k at the pump wavelength and on the slab thickness h. The maximum allowable pump intensities that still do not cause catastrophic events are calculated. The order of failures is determined, i.e., we found the combinations of k and h at which an increase in pumping first causes either breakdown of the AE or boiling of water. It is shown that the STOI effect can occur with both increasing and decreasing optical density if the latter occurs due to a decrease in the slab thickness.

A.N. Alpat'ev, V.A. Smirnov, I.A. Shcherbakov A.M. Prokhorov General Physics Institute, Russian Academy of Sciences, ul. Vavilova 38, 119991 Moscow, Russia; e-mail: lisdenis@mail.ru

Received 3 July 2009
Kvantovaya Elektronika **40** (1) 35 – 39 (2010)
Translated by M.N. Basieva

2. Transverse pumping scheme. Function of heat sources

Figure 1 shows the optical scheme of pumping of an AE. The steady-state selective pumping is performed along the z axis from the two sides of the slab. The pump intensity from each side comprises half the total intensity I_0 (symmetric double-sided pumping) and is uniformly distributed along the x and y axes. Cavity mirrors with the reflection coefficient R at the pump wavelength return the unabsorbed pump radiation back to the AE. The absorption coefficient k of the AE at the pump wavelength is uniform over the entire thickness h of the slab, which is possible at a pump intensity exceeding or equal to the threshold value. Thus, the total pump intensity inside a slab can be written as a function of the z coordinate by the expression

$$I(z) = A_1 \frac{I_0}{2}\{[\exp(-kz) + R\exp(kz - 2kh)] + \exp(-kh)[\exp(kz) + R\exp(-kz)]\}, \quad (1)$$

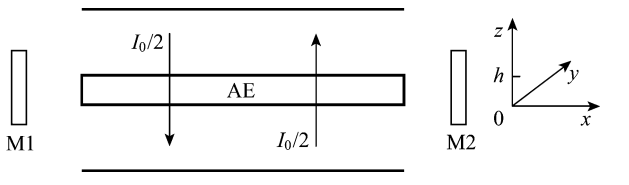

Figure 1. Optical scheme of transverse pumping (M1 and M2 are the cavity mirrors).

where $A_1 = [1 - R^n\exp(-nkh)]/[1 - R^2\exp(-2kh)]$; and n is the number of passes of pump radiation in the slab.

At $R = 1$ and $n \to \infty$, expression (1) is reduced to the form

$$I(z) = \frac{I_0}{2}\frac{\cosh[k(z-h)] + \cosh(kz)}{\sinh(kh)}, \quad (2)$$

and the pump radiation in this case is completely absorbed due to the infinite number of passes. Distribution (2) is similar to the distribution of pump energy absorbed in the AE. From (2), we derive the function describing the distribution of heat sources in the form

$$q_v(z) = \frac{\xi I_0 k}{2}\frac{\cosh(kz - D/2)}{\sinh(D/2)}, \quad (3)$$

where ξ is the fraction of the absorbed pump energy converted to heat and $D = kh$ is the slab optical density at the pump wavelength.

Expression (3) for the function of heat sources under selective pumping can be generalised to the case of broadband lamp pumping. In this case, I_0 corresponds to the total lamp radiation intensity and k is the spectrally averaged absorption coefficient [1–4]. It is obvious that the thermal component ξ in the case of lamp pumping will differ from ξ for selective pumping. The expression derived from (3) taking into account these replacements will exactly coincide with the function of heat sources obtained in [1–4] by a somewhat different method.

3. Thermal conductivity equation. Temperature distribution in the AE. Internal and external temperature differences

Let us consider the temperature distribution in a slab under symmetric double-sided uniform pumping for the above-given optical scheme when cooling (by, for example, running water) is also symmetric, i.e., occurs from two sides, at $z = 0$ and $z = h$, and the slab faces are heat-insulated.

The thermal conductivity equation for this pumping scheme has the form [5–7]

$$\frac{d^2T(z)}{dz^2} = -\frac{q_v(z)}{\lambda},$$

where λ is the thermal conductivity coefficient, the third-kind boundary conditions are

$$\left.\frac{dT(z)}{dz}\right|_{z=0} = \frac{\alpha}{\lambda}[T(0) - T_f], \quad \left.\frac{dT(z)}{dz}\right|_{z=h} = -\frac{\alpha}{\lambda}[T(h) - T_f];$$

α is the coefficient of heat exchange between the slab and water; $T(0)$ and $T(h)$ are the temperatures of the slab side faces at $z = 0$ and $z = h$; and T_f is the temperature of the cooling water.

Since the problem is completely symmetric, i.e., the pump radiation intensities and the slab cooling conditions are identical for both sides, we have $T(0) = T(h)$. Then, the temperature distribution in the slab will have the form

$$T(z) = \frac{\xi I_0}{2\lambda k}\frac{\cosh(D/2) - \cosh(kz - D/2)}{\sinh(D/2)} + \frac{\xi I_0}{2\alpha} + T_f. \quad (4)$$

The first term in (4) [we denote it as $\Delta T_1(z)$] describes the temperature difference inside the slab and coincides with that obtained in [1–4], and the second term (denoted as ΔT_2) describes the difference between the temperature of the slab side surface and the temperature of the cooling medium. It is clear that, if the sum of the temperature difference ΔT_2 and the temperature of cooling water reaches 100 °C, the water will boil. This causes vaporisation and sharply weakens the heat exchange, which, in turn, increases the temperature of the side surface and the internal temperature difference and, as a final result, catastrophically deteriorates the cooling regime. Then, the critical pump intensity causing water to boil is

$$I_0^{cr} = \frac{2\alpha}{\xi}\Delta T_2^{cr}. \quad (5)$$

It is of interest to consider the dependence of temperature difference on the parameters h and D or k and D. Therefore, to analyse the temperature properties of the slab as functions of these parameters, below we will write the expression for $\Delta T_1(z)$ in two ways.

Under arbitrary pumping, the maximum temperature difference (at $z = h/2$) with respect to the temperature of the slab surface (at $z = 0$ or $z = h$) is

$$\Delta T_1^{max} = \begin{cases} AI_0 h\dfrac{\Theta(D)}{D}, \\ AI_0\dfrac{1}{k}\Theta(D), \end{cases} \quad (6)$$

where $A = \xi/(2\lambda)$ and $\Theta(D) = \tanh(D/4)$.

Introducing a variable χ determined from the relation $z = h(\chi + 1)/2$, the difference $\Delta T_1(z)$ can be written by the expression

$$\Delta T_1(z) = \Delta T_1(\chi) = \Delta T_1^{max} f(\chi, D),$$

where $\chi = z/(h/2) - 1$,

$$f(\chi, D) = \frac{\cosh(D/2) - \cosh(\chi D/2)}{\cosh(D/2) - 1}$$

describes the profile of the temperature difference distribution inside the sample over χ normalised to ΔT_1^{max}, and $D/2$ characterises the degree of smoothing of the function $f(\chi, D)$. The dependence $f(\chi, D)$ shown in Fig. 2 is trans-

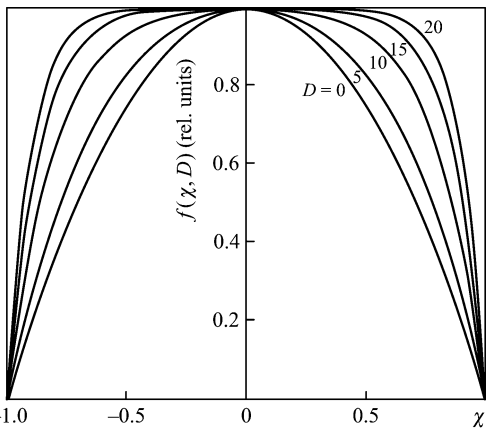

Figure 2. Profiles of the internal temperature difference distribution normalised to ΔT_1^{max} in slabs with different optical densities.

formed into parabolic with decreasing D and into a shell-like distribution with increasing D:

$$f(\chi, D) = \begin{cases} 1-\chi^2, & D \to 0, \\ 1, & D \to \infty. \end{cases}$$

Thus, the smoothing of thermooptical inhomogeneities inside the slab is characterised by two main parameters, namely, by the maximum temperature difference $\Delta T_1^{\max}$ and by the normalised function of temperature distribution over the slab thickness $f(\chi, D)$.

Figure 3 shows the calculated maximum internal temperature difference $\Delta T_1^{\max} = \Delta T_1^{\rm cr}$ in the crystal as a function of the optical density at the critical pump intensity $I_0^{\rm cr}$ that causes boiling of the cooling water. Hereinafter, the parameters used for calculations correspond to the Nd:YAG crystal: $\lambda = 0.13$ W cm^{-1} K^{-1}, $\xi = 0.24$ (for selective pumping at a wavelength of ~ 808 nm), and $\alpha = 1$ W cm^{-2} K^{-1} [8, 9].

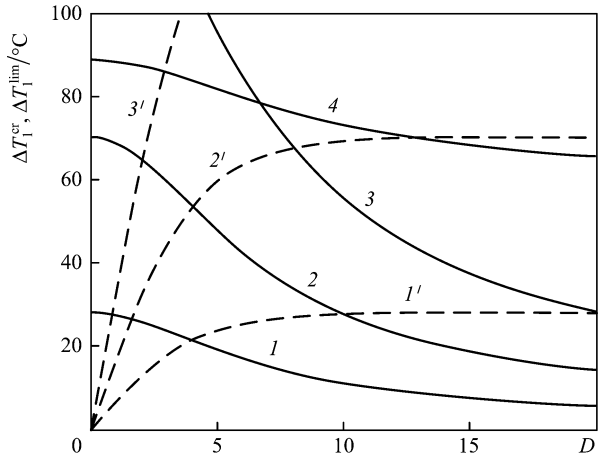

Figure 3. Dependences of the critical ($\Delta T_1^{\rm cr}$) (*1–3*, *1′–3′*) and limiting ($\Delta T_1^{\rm lim}$) (*4*) internal temperature difference in a Nd:YAG slab on the optical density calculated at $h_i = 0.2$ (*1*), 0.5 (*2*), and 1 cm (*3*) and $k_j = 20$ (*1′*), 8 (*2′*), and 4 cm^{-1} (*3′*). The h_i and k_j parameters are bound by the relation $h_i k_j = 4$ at $i = j$.

Curves (*1*), (*2*), and (*3*) are plotted for constant thicknesses h (h_i, $i = 1, 2, 3$), while curves (*1′*), (*2′*), and (*3′*) are calculated for constant k (k_j, $j = 1, 2, 3$), the values of constant h and k being chosen so that $h_i k_j = 4$ at $i = j$. Then, $\Delta T_{1i}^{\rm cr}|_{D\to 0} = \Delta T_{1i}^{\rm cr}|_{D\to\infty}$. One can see from Fig. 3 that $\Delta T_1^{\rm cr}$ decreases both with increasing and decreasing optical density D, as D increases at $h = \text{const}$, $D = \text{const}$ with decreasing h and increasing k, and D decreases with $k = \text{const}$. In all the three cases, the thermooptical inhomogeneities are smoothed due to a decrease in the maximum internal temperature difference. However, the STOI effect is most pronounced in the first case, because, in addition to a decrease in $\Delta T_1^{\max}$, the normalised temperature difference distribution $f(\chi, D)$ is also smoothed. The occurrence of the STOI effect at $h = \text{const}$ and increasing D was experimentally confirmed in [4, 10] by a decrease in the laser radiation divergence.

4. Distribution of thermoelastic stresses in the slab

The expression for thermoelastic stresses in a slab with the internal temperature distribution $T(z)$ was obtained, for example, in [11, 12]:

$$\sigma(z) = \gamma\left[-T(z) + \bar{T} + \overline{T(z)(z-h/2)}\right], \tag{7}$$

$$\sigma_{xx}(z) = \sigma_{yy}(z) = \sigma(z), \quad \sigma_{zz} = 0,$$

where

$$\bar{T} = \frac{1}{h}\int_0^h T(z)\mathrm{d}z;$$

$$\overline{T(z)\left(z-\frac{h}{2}\right)} = \frac{12}{h^3}\left(z-\frac{h}{2}\right)\int_0^h T(z)\left(z-\frac{h}{2}\right)\mathrm{d}z;$$

γ is a coefficient proportional to the thermal expansion coefficient and inversely proportional to the elastic compliance coefficient, which changes depending on the slab orientation with respect to the crystallographic axes of the crystal [4].

Substituting temperature from (4) into expression (7), we find the stress distribution over the slab thickness similar to the expression given in [4],

$$\sigma(z) = \gamma\frac{\xi I_0 h}{4\lambda}\,\frac{(D/2)\cosh(kz - D/2) - \sinh(D/2)}{(D/2)^2\sinh(D/2)}. \tag{8}$$

To prevent breakdown of the slab with heating, it is necessary to hold the inequality $\sigma(z) \leqslant \sigma_{\rm s}$, where $\sigma_{\rm s}$ is the critical cleavage stress (for YAG crystals with the orientation z || [100], $\sigma_{\rm s} = 2008$ kg cm^{-2} and $\gamma = 33.95$ kg cm^{-2} K^{-1} [4]). Under stressed conditions, inside the slab there are two symmetrically lying relief planes, which are parallel to the wide surfaces of the slab. The stress is negative (pressing) between the relief planes and positive (stretching) between the relief planes and the slab surfaces.

At any values of parameters k and h, the maximum stresses $\sigma(z)$ appear at the surfaces with $z = 0$ and $z = h$. The limiting pump intensity at which the slab is destroyed is estimated as

$$I_0^{\rm lim} = \begin{cases} BD\Omega(D)/h, \\ Bk\Omega(D), \end{cases} \tag{9}$$

where

$$B = \frac{\sigma_{\rm s}\lambda}{\gamma\xi}; \quad \Omega(D) = \frac{D\sinh(D/2)}{(D/2)\cosh(D/2) - \sinh(D/2)}.$$

Figure 4 shows the calculated limiting pump intensity $I_0^{\rm lim}$ (at a wavelength of ~ 808 nm), which causes the thermal breakdown of the slab, versus the optical density. Each of the curves (*1*), (*2*), (*3*) is calculated for a constant thickness h (h_i, $i = 1, 2, 3$), and each of the curves (*1′*), (*2′*), (*3′*) is plotted for a constant coefficient k (k_j, $j = 1, 2, 3$). The values of k and h are chosen so that $h_i k_j = 6$ at $i = j$. In this case, $I_{0i}^{\rm lim}|_{D\to 0} = I_{0i}^{\rm lim}|_{D\to\infty}$. Figure 4 shows that $I_0^{\rm lim}$ increases both with increasing and decreasing optical density, as D increases with $h = \text{const}$, $D = \text{const}$ with decreasing h and increasing k, and D decreases with $k = \text{const}$. In all three cases, the threshold intensity corresponding to the thermal breakdown of the slab increases. An experimental proof of this STOI effect at $h = \text{const}$ and increasing k is given in [4, 10].

The limiting internal temperature difference at the instant of breakdown is found from (6) and (9) as

$$\Delta T_1^{\rm lim} = \frac{\sigma_{\rm s}}{2\gamma}\Psi(D), \tag{10}$$

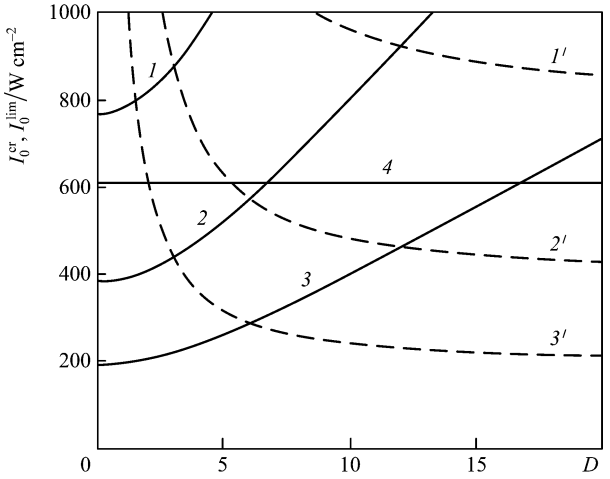

Figure 4. Dependences of the limiting ($I_0^{\lim}$) (*1–3*, *1′–3′*) and critical (I_0^{cr}) (*4*) intensities of selective (808 nm) pumping of a Nd : YAG slab on its optical density calculated at $h_i = 0.5$ (*1*), 1 (*2*), and 2 cm (*3*) and $k_j = 12$ (*1′*), 6 (*2′*), and 3 cm^{-1} (*3′*). The h_i and k_j parameters are bound by the relation $h_i k_j = 6$ at $i = j$.

where

$$\Psi(D) = \Theta(D)\Omega(D) = \frac{D[\cosh(D/2) - 1]}{(D/2)\cosh(D/2) - \sinh(D/2)};$$

$$\lim_{D\to 0} \Psi(D) = 3, \ \lim_{D\to\infty} \Psi(D) = 2.$$

One can see that $\Delta T_1^{\lim}$, in contrast to $\Delta T_1^{\max} = \Delta T_1^{cr}$ and $I_0^{\lim}$, depends only on the optical density.

The limiting internal temperature difference integral-averaged over the thickness at the instant of breakdown is determined from (4) and (9):

$$\overline{\Delta T_1^{\lim}} = \frac{1}{h}\int_0^h \Delta T_1(z)\,\mathrm{d}z = \frac{\sigma_s}{2\gamma}\bar{\Psi}, \qquad (11)$$

where $\bar{\Psi} = 2$.

The limiting internal temperature difference in a Nd : YAG crystal at the instant of breakdown as a function of the optical density is shown in Fig. 3.

Thus, we obtained the dependences of the maximum internal temperature difference in a slab pumped with different intensities on the optical density, as well as on each of the k and h parameters separately. From Figs 3 and 4, one sees that there exists a particular order at which the internal temperature difference reaches its either critical or limiting calculated value with increasing pump intensity, which depends on the values of the k and h parameters.

5. Regions of optical densities corresponding to boiling of water or to breakdown of the AE

If the equality $I_0^{\lim} = I_0^{cr}$ is valid, the limiting internal temperature difference $\Delta T_1^{\lim}$ is reached simultaneously with the critical external temperature difference ΔT_2^{cr}. This is possible only at a particular combination of the k and h parameters, which is determined from the following equation found by equating expressions (5) and (9):

$$\frac{D\Omega(D)}{h} = \frac{2\alpha\Delta T_2^{cr}\gamma}{\lambda\sigma_s}. \qquad (12)$$

Note that Eqn (12) does not contain ξ. Therefore, the k and h parameters that satisfy Eqn (12) can be exist for different pumping methods, for example, lamp or selective pumping.

Let us take into account the temperature dependence of λ. To do this, we use the data given for YAG in, for example, [13]:

$$\lambda(T) = \lambda_0\left(\frac{204K}{T - 96K}\right)^{0.63}, \qquad (13)$$

where λ_0 is the thermal conductivity coefficient at $T = 300$ K.

To determine λ, we will use two values of the temperature T in formula (13), the maximum limiting and the limiting integral-averaged over the thickness, at which the slab breakdown and water boiling occur simultaneously:

$$T_{\max}^{\lim}(D) = \frac{\sigma_s}{2\gamma}\Psi(D) + 100\,^{\circ}\mathrm{C}, \qquad (14)$$

$$\overline{T_{\max}^{\lim}} = \frac{\sigma_s}{\gamma} + 100\,^{\circ}\mathrm{C}. \qquad (15)$$

We assume that the thermal conductivity coefficient is constant over the entire slab thickness. The calculation with the use of the two temperatures, $T_{\max}^{\lim}$ and $\overline{T_{\max}^{\lim}}$, allows us to more reliably estimate the sought relation between the k and h parameters.

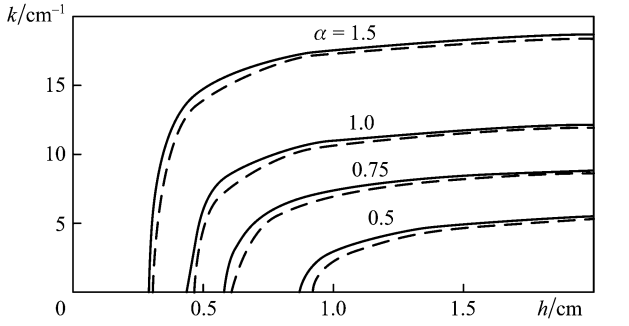

Figure 5. Lines dividing the (h, k) plane into regions corresponding to different events occurring with increasing the pump intensity: destruction of the sample (to the right of each line) or boiling of water (to the left). The calculations are performed for an YAG crystal with the orientation $z \,||\, [100]$. The solid and dashed curves are calculated for the thermal conductivity coefficients λ corresponding to $T_{\max}$ and $\bar{T}_{\max}$, respectively.

Figure 5 presents the calculated curves that divide the plane (h, k) into regions in which an increase in the pump intensity first causes either boiling of water (to the left of each curve) or breakdown of the slab (to the right of each curve). It is obvious that the maximum temperature of the slab at the boundaries of the regions is determined by expression (14), i.e., it is $\sim$190 °C at $D \to 0$ and decreases to $\sim$160 °C at higher D.

6. Conclusions

In this work, we studied the specific features of thermal regimes in water-cooled rectangular laser slabs under steady-state pumping.

(i) It is shown that, with increasing optical density of the slab, along with the STOI effect, there exists the anti-STOI effect, which manifests itself depending on the relation

between the h and k parameters. For example, increasing the optical density at $h = \text{const}$, we obtain the STOI effect, while the anti-STOI effect is observed if the optical density is increased at $k = \text{const}$ (due to an increase in the maximum internal temperature difference and a decrease in the threshold of the thermal breakdown of the crystal under action of optical pumping).

(ii) The dependence of the maximum internal temperature difference on the optical density at the instant of the slab breakdown is determined. With increasing optical density, this difference decreases no more than by 1/3 of its value at low optical densities.

(iii) The plane (k, h) is divided into two regions that differ by the first event occurring with increasing the pump intensity – destruction of the slab or boiling of water. It is shown that the position of the boundary between the regions does not depend on the fraction of absorbed pump energy converted to heat. Thus, the calculated results can be applied for any pumping method, both for the lamp (broadband spectrum) and diode (narrow selective spectrum) pumping.

(iv) For a crystal with thermomechanical parameters corresponding to the YAG crystal, it is shown that the maximum temperature of the slab in each of the two regions cannot exceed 190 °C at low optical densities and 160 °C at higher optical densities without damage to the crystal. These limiting temperatures are reached at the boundary between the two regions, i.e., at k and h at which the breakdown of the slab and boiling of water occur simultaneously.

References

1. Danilov A.A., Osiko V.V., Prokhorov A.M., Shcherbakov I.A. *Kvantovaya Elektron*., **15** (3), 486 (1988) [*Sov. J. Quantum Electron*., **18** (3), 307 (1988)]; Preprint IOFAN, No. 23 (Moscow, 1987).
2. Danilov A.A., Nikol'skii M.Yu, Shcherbakov I.A. *Izv. Akad. Nauk SSSR. Ser. Fiz*., **51**, 1431, (1987).
3. Prokhorov A.M., Shcherbakov I.A. *Izv. Akad. Nauk SSSR. Ser. Fiz*., **51**, 1341 (1987).
4. Alpat'ev A.N., Danilov A.A., Nikol'skii M.Yu, Prokhorov A.M., Tsvetkov V.B., Shcherbakov I.A. *Trudy IOFAN*, **26**, 107 (1990).
5. Mikheev M.A. *Osnovy teploperedachi* (Heat-Transfer Principles) (Moscow – Leningrad: Gosenergoizdat, 1956).
6. Carslaw H.S., Jaeger J.C. *Conduction of Heat in Solids* (New York, Oxford University Press, 1959; Moscow: Nauka, 1964).
7. Lykov A.V. *Theoriya teploprovodnosti* (Theory of Heat Conduction) (Moscow: Vysshaya shkola, 1967).
8. Zverev G.M., Golyaev Yu.D., Shalaev E.A., Shokin A.A. *Lazery na alyumoittrievom granate s neodimom* (Lasers Based on Neodymium-doped Aluminum Yttrium Garnet) (Moscow: Radio I svyaz', 1985).
9. Belostotzkii B.R., Lyubavskii Yu.V., Ovchinnikov V.M. *Osnovy lazernoi tekhniki* (Principles of Laser Engineering) (Moscow: Sov. radio, 1972).
10. Danilov A.A., Nikol'skii M.Yu, Prokhorov A.M., Tsvetkov V.B., Shcherbakov I.A. *Kvantovaya Elektron*., **16** (3), 517 (1989) [*Sov. J. Quantum Electron*., **19** (3), 342 (1989)].
11. Mezenov A.V., Soms L.N., Stepanov A.I. *Termooptika tverdotel'nykh lazerov* (Thermooptics of Solid-State Lasers) (Leningrad: Mashinostroenie, 1986).
12. Indenbom V.L., Sil'verstova I.M., Sirotin Yu.I. *Kristallografiya*, **1**, 599 (1956).
13. Contag K., Erhard S., Giesen A., in *Trends in Optics and Photonics* (Washington, DC, Optical Society of America, 2000) Vol. 34, pp 124 – 130.